THE ASTROPHYSICAL JOURNAL, 466:742–749, 1996 August 1

VISIBLE AND FAR-ULTRAVIOLET WFPC2 IMAGING OF THE NUCLEUS OF THE GALAXY NGC 205[1]

D. HEATH JONES,[2] JEREMY R. MOULD,[2] ALAN M. WATSON,[3] CARL GRILLMAIR,[4] JOHN S. GALLAGHER III,[5] GILDA E. BALLESTER,[6] CHRISTOPHER J. BURROWS,[7] STEFANO CASERTANO,[8] JOHN T. CLARKE,[6] DAVID CRISP,[4] RICHARD E. GRIFFITHS,[8] J. JEFF HESTER,[9] JOHN G. HOESSEL,[5] JON A. HOLTZMAN,[3] PAUL A. SCOWEN,[9] KARL R. STAPELFELDT,[4] JOHN T. TRAUGER,[4] AND JAMES A. WESTPHAL[10]

Received 1995 August 28; accepted 1996 February 6

ABSTRACT

We have imaged the nucleus of NGC 205 through the F555W and F160BW filters of WFPC2 on the high-resolution planetary camera (PC). The nucleus consists of a resolved cluster of stars extending $7'' \times 6''$.

The projected radial distribution of surface brightness can be fitted by a Hubble law with a small core of FWHM 214 × 190 mas (0.74 × 0.66 pc). We find that the nucleus of NGC 205 shares a number of characteristics with globular clusters. Absolute photometry is also presented in a half-arcsec aperture and is found to verify the amount of UV upturn observed in the spectral energy distribution of the nucleus by others (e.g., Bertola et al. 1995).

Of the hypotheses available to explain the origin of the nucleus, the observations are most consistent with its being an intermediate age cluster. The most likely scenarios are that it is a either a star cluster whose orbit has decayed—therefore drawing it to rest at the galaxy center—or a cluster that has formed as the repository of the gas from generations of star formation.

Together with the ground-based measurement of a low-velocity dispersion, the small core radius implies a 10^7 yr relaxation time, suggesting the cluster core may have collapsed. An upper limit of $9 \times 10^4\ M_\odot$ can be put on the mass of any central black hole.

Subject headings: galaxies: individual (NGC 205) — galaxies: nuclei — galaxies: stellar content — ultraviolet: stars

1. INTRODUCTION

The nuclei of galaxies remain an area of intense interest, both structurally and as regards the stellar population of which nuclei are composed. The structure and kinematics of galactic nuclei have recently been reviewed by Kormendy & Richstone (1995). In dwarf elliptical galaxies, the presence of nuclei is a common, but not universal, phenomenon. For instance, Binggeli, Sandage, & Tammann (1985) have found that a large fraction of early type dwarfs (dE and dS0 types) in the Virgo Cluster contain an unresolved, starlike central nucleus. Furthermore, the frequency of nucleation is found to decline with decreasing luminosity (Sandage, Binggeli, & Tammann 1985).

NGC 205 is a dwarf elliptical[11] companion of M31. With *HST*, M31 and its companions offer us a unique opportunity to study galaxy nuclei at high spatial resolution (Lauer et al. 1992, 1993). The star formation history of the galaxy, the prototype of dwarf ellipticals with young stars, is described by Gallagher & Mould (1981) and Hodge (1989). The kinematics of the central region are discussed by Held et al. (1990) and the spectrum of the nucleus by Da Costa & Mould (1988).

Bertola et al. (1995) have observed NGC 205 with the FOC, but in the process of measuring the far-ultraviolet flux they had to modify the FOC calibration. Far-UV measurements with WFPC2 have the advantage of Woods filter protection against red leak. We can therefore verify the FUV/visible flux ratio of the nucleus of NGC 205. We also examine the structure of the nucleus, which is imaged on the PC chip.

2. OBSERVATIONS AND PHOTOMETRY REDUCTION

Two images of the nucleus of NGC 205 were obtained on 1994 September 4 using the PC1 chip of WFPC2: one through the F555W filter (10 s exposure; see Fig. 1) and the other through F160BW (1200 s exposure; see Fig. 2). Bias subtraction, flat-fielding, and cosmic-ray removal were per-

[1] Based on observations with the NASA/ESA *Hubble Space Telescope.*

[2] Mount Stromlo and Siding Springs Observatories, Institute of Advanced Studies, Australian National University, Private Bag, Weston Creek Post Office, ACT 2611, Australia.

[3] Department of Astronomy, New Mexico State University, Box 30001 Department 4500, Las Cruces, NM 88003-8001.

[4] Jet Propulsion Laboratory, 4800 Oak Grove Drive, Mail Stop 179-225, Pasadena, CA 91109.

[5] Department of Astronomy, University of Wisconsin–Madison, 475 N. Charter Street, Madison, WI 53706.

[6] Department of Atmospheric and Oceanic Sciences, University of Michigan, 2455 Hayward, Ann Arbor, MI 48109.

[7] Space Telescope Science Institute, 3700 San Martin Drive, Baltimore, MD 21218.

[8] Department of Astronomy, Johns Hopkins University, 3400 N. Charles St., Baltimore, MD 21218.

[9] Department of Physics and Astronomy, Arizona State University, Tyler Mall, Tempe, AZ 85287.

[10] Division of Geological and Planetary Sciences, California Institute of Technology, Pasadena, CA 91125.

[11] Kormendy (1985) has pointed out that NGC 205 occupies the fundamental plane parameter space for disk rather than elliptical galaxies. This being the case, galaxies such as NGC 205 are frequently described as dwarf *spheroidals* as a means of distinguishing from true low-luminosity ellipticals.

1996ApJ...466..742J

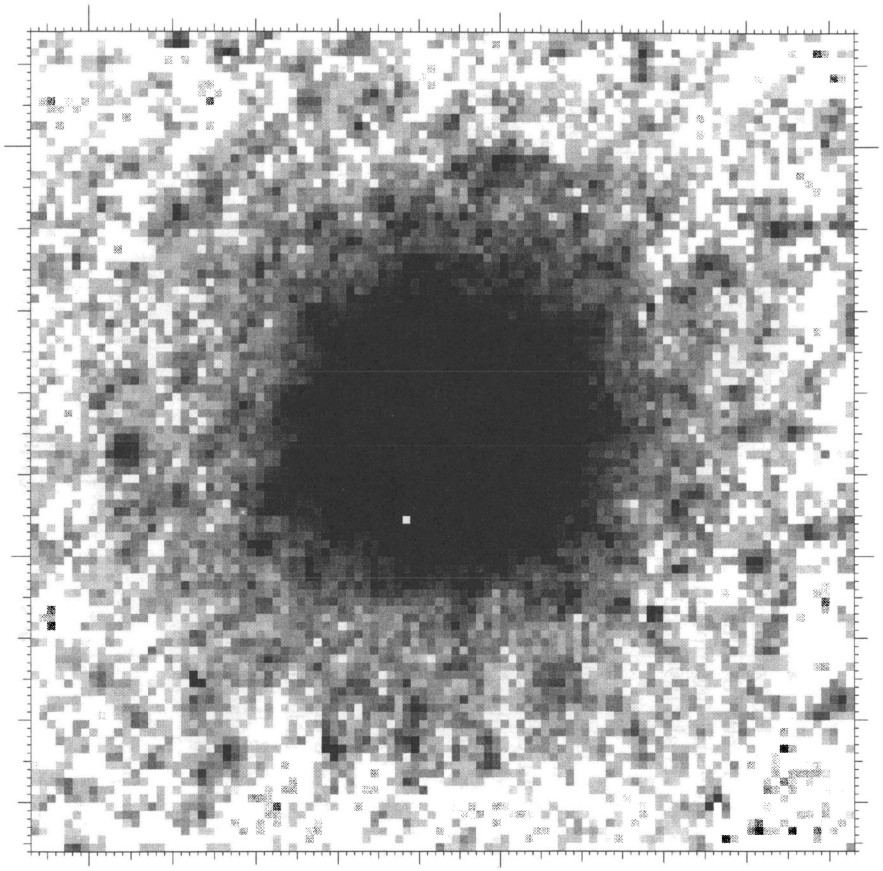

FIG. 1*a*

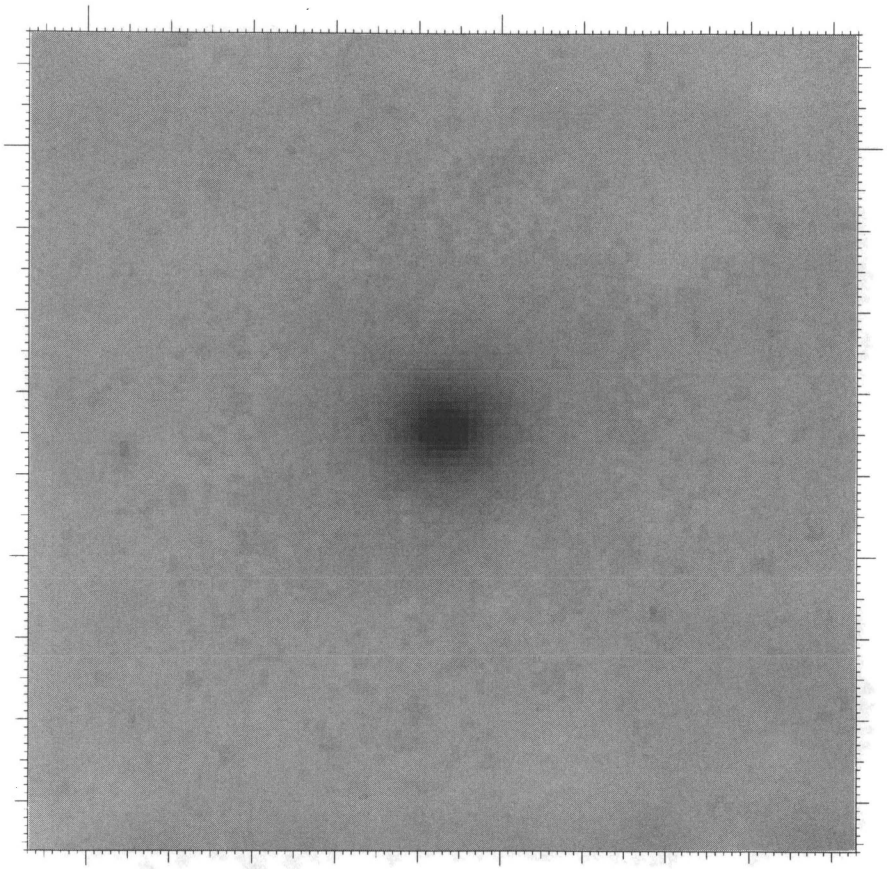

FIG. 1*b*

FIG. 1.—Two versions of the same image of the NGC 205 nucleus under different degrees of stretch to show the (*a*) outlying and (*b*) innermost structure. The image was taken through the F555W filter with PC1 of WFPC2 and is 100 × 100 pixels (4″.55 × 4″.55 = 15.68 × 15.68 pc). Here north is 168° clockwise and the semimajor axis is 8° clockwise from the positive *x*-axis. The image has not been deconvolved with the PSF.

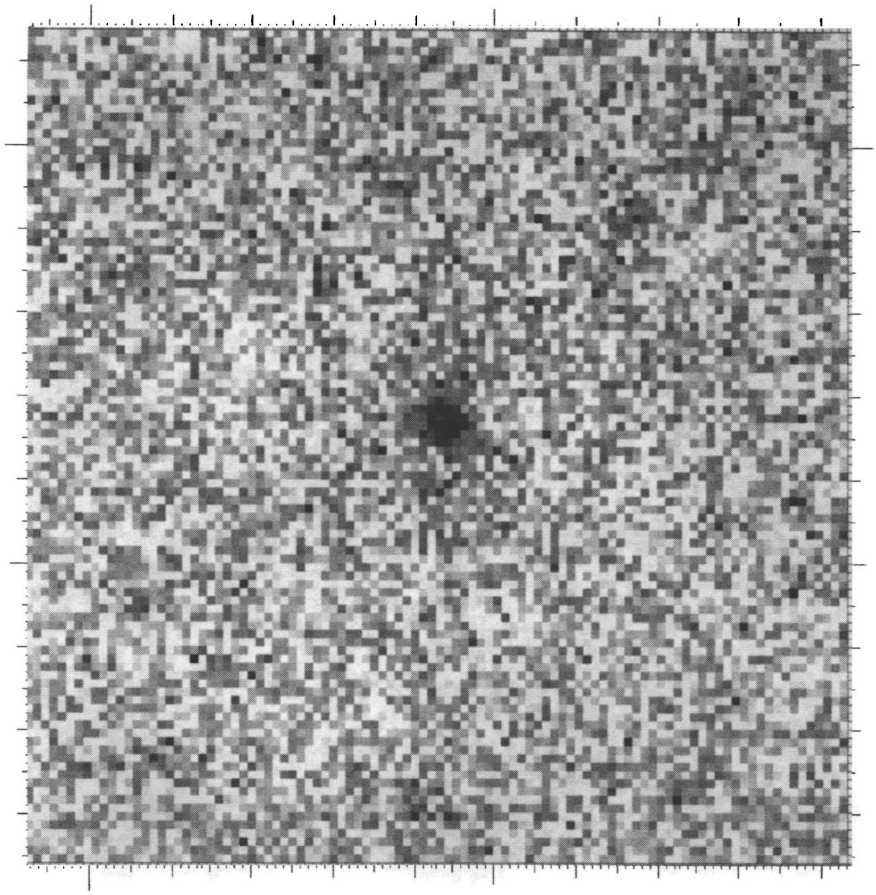

FIG. 2.—Image of the nuclear region of NGC 205 taken with PC1 of the WFPC2 through the F160BW filter. The frame is 100 × 100 pixels (4.″55 × 4.″55 = 15.68 × 15.68 pc). In this figure, north is 168° clockwise and the semimajor axis is 8° clockwise from the positive x-axis. The image has not been deconvolved with the PSF.

formed according to the prescriptions of Holtzman et al. (1995b). The characteristics of the F160WB filter are detailed in Watson et al. (1994), and a full description of WFPC2 can be found in both Trauger et al. (1994) and the instrument handbook (Burrows 1994).

Aperture photometry was performed on each image using a radius $r = 6$ pixels (=0.″273). This was chosen as a compromise between having an aperture sufficiently large to minimize uncertainties due to centroiding but small enough to keep the background noise negligible. Because of the intrinsically low flux of the nucleus through F160BW, accurate aperture centroiding on the nucleus was done from the F555W image. Comparisons between F555W and F160BW images of the globular cluster NGC 7099 taken using PC1, reveal shifts in star centroids of less than ~2 pixels between frames. We then determined that for a 6 pixel radius aperture, the uncertainty in magnitude due to shifts in centroid less than 2 pixels is 0.03 mag in both frames. This is also comparable to the magnitude uncertainty due to the photon sky noise for an aperture of the same size.

2.1. *F555W Photometry Calibration*

Calibration of the F555W photometry was done by combining the equation for calibrating WFPC2 photometry with the STScI magnitude system (Holtzman et al. 1995a),

$$\mathrm{STMAG} = -2.5 \log F_\lambda - 21.1 \quad (1)$$

with that for converting observed WFPC2 count rates into units of STMAG:

$$\mathrm{STMAG} = -2.5 \log [\mathrm{counts}\ (DN/s)] + Z_{\mathrm{STMAG}} + 2.5 \log GR_i\,, \quad (2)$$

as described in § 5.2 of Holtzman et al. (1995a). Here Z_{STMAG} is a filter-dependent magnitude offset and F_λ is the absolute flux from the source (which is assumed to be constant across the filter). GR_i is a quantity used by Holtzman et al. (1995a) to characterize the gain of the CCD.

Upon equating (1) and (2) we obtain the conversion from counts to flux

$$F_\lambda = \frac{\mathrm{counts}\ (DN/s)}{GR_i} \times 10^{-0.4(Z_{\mathrm{STMAG}} + 21.1)}\,, \quad (3)$$

which for the F555W filter becomes

$$F_{555} = \frac{\mathrm{counts}\ (DN/s)}{GR_i} \times (7.67 \times 10^{-18})\,. \quad (4)$$

Here $GR_i = 1$ (for the 14 e^-/DN gain state; Holtzman et al. 1995a) and we have used the value of Z_{STMAG} for F555W from Table 9 of Holtzman et al. (1995a). Once the flux is calibrated (in units of ergs cm^{-2} s^{-1} Å^{-1}), it can be used to yield an apparent magnitude m_λ in the WFPC2 system. We do this by combining equation (3) above with equation (7)

of Holtzman et al. (1995a) to get

$$m_\lambda = -2.5 \log F_\lambda + (Z_{\rm syn} - Z_{\rm STMAG} - 21.1) . \quad (5)$$

Values of $Z_{\rm syn}$ are also listed in Table 9 of Holtzman et al. (1995a) from which we find a zero point of $(Z_{\rm syn} - Z_{\rm STMAG} - 21.1) = -21.07$ for m_V. The results of the F555W calibration are presented in § 2.3.

2.2. *F160BW Photometry Calibration*

We derived our own calibration for the F160BW photometry from the fundamental equation describing photon detection,

$$N_\gamma = A \int_0^\infty \frac{F_\lambda}{h\nu} Q_\lambda T_\lambda d\lambda , \quad (6)$$

where Q_λ and T_λ are the overall system and filter responses, respectively, N_γ is the total number of photons per second, A is the collecting area of the telescope, and $F_\lambda/h\nu$ is the photon flux (photons s^{-1} cm^{-2} nm^{-1}). This was necessary, since the stellar models used in Holtzman et al. (1995a) are not a good match to the spectral energy distribution (SED) of the NGC 205 nucleus compiled by Bertola et al. (1995) and reproduced in Figure 3. When equation (6) is combined with equation (10) of Holtzman et al. (1995b), the flux calibration scaling factor F_{λ_0} can be found according to

$$F_{\lambda_0} = F_\lambda(\lambda_{\rm eff}) \left[\frac{A}{14} \int_0^\infty \frac{F_\lambda}{h\nu} Q_\lambda T_\lambda d\lambda \right]^{-1} , \quad (7)$$

where the factor of 14 accounts for the CCD gain (14 DN/e). Here $F_\lambda(\lambda_{\rm eff})$ is the flux at the effective wavelength $\lambda_{\rm eff}$ of F160BW, defined by

$$\lambda_{\rm eff} = \frac{\int_0^\infty (F_\lambda/h\nu) Q_\lambda T_\lambda \lambda d\lambda}{\int_0^\infty (F_\lambda/h\nu) Q_\lambda T_\lambda d\lambda} . \quad (8)$$

Taking F_λ from the NGC 205 SED used by Bertola et al. (1995) we evaluated $\lambda_{\rm eff}$ for the F160BW filter using Q_λ data from J. Holtzman (1995) and the T_λ data of Burrows (1994). The resulting effective wavelength ($\lambda_{\rm eff} = 156$ nm) was used then to find the $F_\lambda(\lambda_{\rm eff})$ value of the Bertola et al. (1995) SED and thus determine F_{λ_0} ($= 1.18 \times 10^{-14}$ erg cm^{-2} s^{-1} $Å^{-1}$) using equation (7). F_{λ_0} was used consequently to calibrate our photometry through

$$F_{160} = F_{\lambda_0} \times \frac{\text{counts } (DN/s)}{GR_i} . \quad (9)$$

Here $GR_i = 1.987$, which is the value for the PC1 chip when read through bay 4 of the WFPC2 camera (Holtzman et al. 1995a) and $F_{\lambda_0} = 1.2 \times 10^{-14}$ erg cm^{-2} s^{-1} $Å^{-1}$.

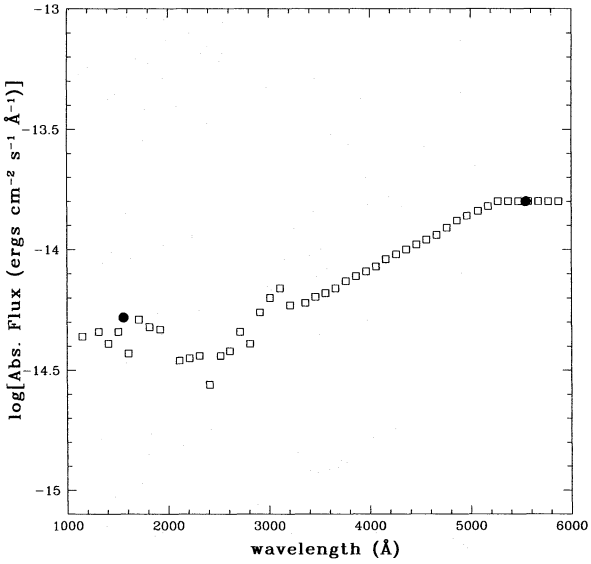

FIG. 3.—Photometry of the nucleus of NGC 205 in F160BW and F555W (*solid circles*) compared with the spectral energy distribution (SED) compiled by Bertola et al. (*open squares*). The F160BW and F555W fluxes have been scaled with respect to the SED at 5550 Å.

2.3. *Results*

Before the photometric calibration, raw magnitudes were corrected for interstellar extinction by $A(555) = 0.11$ and $A(156) = 0.29$ mag in F555W and F160BW, respectively (where 156 nm is the effective wavelength). These extinctions were determined from the analytic expression of Cardelli, Clayton, & Mathis (1988) for $A(\lambda)/A(V)$ computed with coefficients from Cardelli, Clayton, & Mathis (1989). The amount of blue extinction to NGC 205 listed in Burstein & Heiles (1984) [$A(B) = 0.14$] was used with equations (4) and (9). These were applied to obtain photometrically calibrated fluxes F_{555} and F_{160} for the nucleus over the aperture.

Further corrections were required for two important effects associated with the WFPC2 camera (Holtzman et al. 1995b): (1) UV-absorbing contaminants that slowly build up on the CCD window over several weeks as the chip is kept at operating temperature (currently −88° C), and (2) a small amount of flux loss due to a charge transfer problem with the CCD. The correction for contaminant buildup depends on the size of the UV component of the light and the time between observation and the previous decontamination, which is achieved by warming the CCD . The present observations occurred 8 days following the standard decontamination of 1994 August 27 (Holtzman et al. 1995a). Using equation (1) of Holtzman et al. (1995a) with the contamination rate for chip 1 given therein, this amounts to a flux correction by a factor of 1.089 in F160BW alone. The correction for charge loss during transfer depends on the location of the nucleus on the chip and requires compensation by a factor of 1.028 in both filters. This was derived from the simple correction procedure given by Holtzman et al. (1995b).

Applying the corrections outlined above gives absolute flux measures of $F_{555} = 1.83 \times 10^{-15}$ erg cm^{-2} s^{-1} $Å^{-1}$ and $F_{160} = 6.05 \times 10^{-16}$ erg cm^{-2} s^{-1} $Å^{-1}$ over a 0.″273 radius aperture. The flux ratio we measure between these two wavelengths agrees with that found in the SED compiled by Bertola et al. (1995) for NGC 205 to within ~20% (Fig. 3). Given the low signal-to-noise ratio of the F160BW image we have not looked for a color gradient in the nucleus. By equation (5) we determine the NGC 205 nucleus to have apparent V magnitude $\hat{m}_V = 15.77$ over the 0.″273 aperture.

We estimate from the F555W image that the nucleus extends at its fullest approximately 7″ × 6″. Photometry over an aperture of this size (radius 70 pixels) gives a total apparent V magnitude of $m_V = 14.57$ (after applying the corrections). At a distance of 720 kpc (Mould, Kristian, & Da Costa 1984) this implies a total absolute V magnitude of $M_V = -9.6$. This is comparable with the absolute visual

magnitudes of the brightest galactic globular clusters in the catalog of Djorgovski (1993).

3. NUCLEUS MORPHOLOGY

In determining the core structure, we convolved a model nucleus with the PSF for the WFPC2 (Krist & Burrows 1995) and applied a χ^2 minimization technique to find the best fit to the observational data (over a 0".23 radius aperture).

We used a model of the modified Hubble form

$$I(x, y) = I_0\left[1 + \left(\frac{r}{r_0}\right)^2\right]^{-1}, \quad (10)$$

where

$$\frac{r}{r_0} = \sqrt{\left(\frac{\hat{x}}{a}\right)^2 + \left(\frac{\hat{y}}{b}\right)^2}, \quad (11)$$

and

$$\hat{x} = (x - x_c)\cos\theta + (y - y_c)\sin\theta, \quad (12)$$

$$\hat{y} = -(x - x_c)\sin\theta + (y - y_c)\cos\theta, \quad (13)$$

which describes concentric elliptical isophotes of semimajor and semiminor axes a and b, respectively. Here I_0 is the peak intensity found at the model center (x_c, y_c) and θ is the angle measured clockwise from the y axis to the semimajor axis. In fitting the model to the observed data we set $r_0 = b$. This modifies the isophote semimajor and semiminor axes to $A = af$ and $B = bf$, respectively, where f is an expression of the isophote intensity such that $I = I_0/(f^2 + 1)$. At $I = I_0/2, f = 1$ and so we define our FWHM dimensions of the model as $2a \times 2b$. In determining a core radius r_c we will use half of the mean FWHM.

The χ^2 minimization procedure was initiated by minimizing χ^2 for a, θ, and b individually, rather than for all three parameters simultaneously. An additional iteration of the minimization was then performed by varying a (and hence b) with fixed axis ratio and θ. No model corrections were made for image distortions (Holtzman et al. 1995b), since the area covered by the nucleus is small compared to that of the total PC1 chip area.

Previous studies of the core structure of the NGC 205 nucleus have found it to be slightly elongated and barely resolved with axis ratio $q = 0.83$ (Bertola et al. 1995). We find our measurement of $q = 0.89 \pm 0.06$ is close to this. Our model of best fit uses $a = 107 \pm 3$ mas and $b = 95 \pm 3$ mas. Thus, the $I = I_0/2$ isophote has semimajor and semiminor axes of $A = 107 \pm 3$ mas (0.37 ± 0.01 pc) and $B = 95 \pm 3$ mas (0.33 ± 0.01 pc), respectively. We also find that the nucleus is oriented $160° \pm 30°$ east of north, which is parallel to the 170° east of north position angle measured for the galaxy (Nilson 1973) to within the estimated uncertainty. The uncertainties listed here correspond to scatter in χ^2 of approximately $\pm 11\%$ in θ and $\pm 3\%$ in a and b. The large uncertainty in the nucleus position angle is due to its small eccentricity. Figure 4 shows a contour plot of the model that best fits the NGC 205 nucleus.

The results of the parameter fit give the nucleus a FWHM of 214 × 190 mas (0.75 × 0.66 pc) and thus a core radius r_c of 100 mas (0.35 pc). This places the nucleus slightly smaller than the average for core radii of galactic globular clusters (catalog of Djorgovski 1993). Figures 5 and 6 show the normalized radial profiles for both the model and observed nuclei in the F555W filter, as well as that of the PSF. The value of r_0 is model dependent in the sense that, if we fit a modified Hubble profile with an outer power of -2 (instead of -1), r_0 is larger by a factor of almost 2. But the FWHM of the core (r_c) is not greatly changed by such a model substitution.

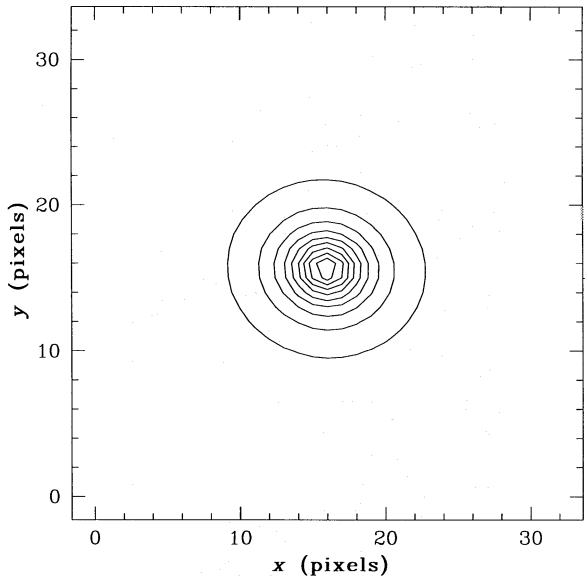

FIG. 4.—Contour plot of the nuclear model of best fit (before convolution with the PSF). The contour interval is 485 counts and the data range between 44 and 4894 counts.

We have also performed a formal deconvolution of the nucleus with 20 Lucy-Richardson iterations to obtain the major axis profile shown in Figure 7. In Table 1, r is in arcsec and μ_V in mag arcsec^{-2}. The convolution and the deconvolution are in generally good agreement, with the distinction that the convolution assumes a flat core, whereas the deconvolution deduces rising surface bright-

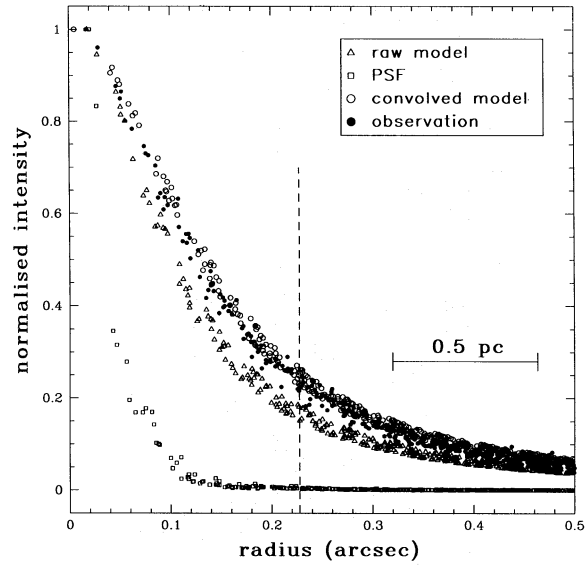

FIG. 5.—Normalized radial profiles of the model nucleus before convolution (*open triangles*), point spread function (*open squares*), model nucleus after convolution (*open circles*), and the observed nucleus (*solid circles*). Note that these profiles are the plot of all pixels in each image and not a two-dimensional slice taken in a particular direction. The dashed vertical line indicates the aperture radius over which χ^2 was minimized.

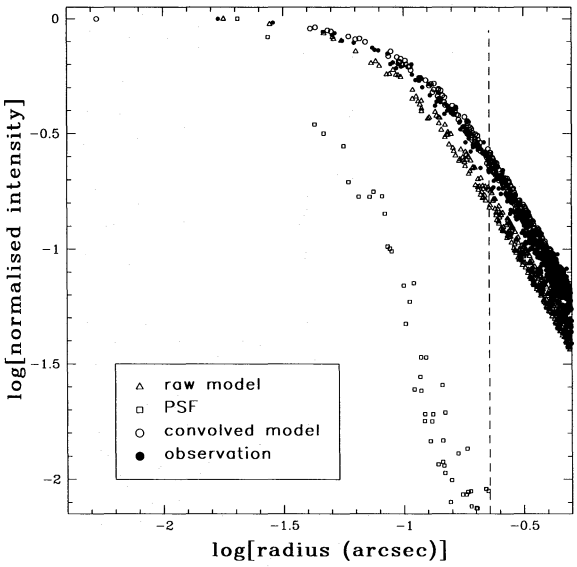

FIG. 6.—Same data as that of the previous figure except on a logarithmic scale. The dashed vertical line indicates the aperture radius over which χ^2 was minimized.

ness as r goes to zero. At $r \approx 0''.06$ ($0.6r_c$) the slope of the deconvolved surface brightness power law is $\gamma = -0.68$. This may be compared with $\gamma \approx -0.4$ for the globular cluster M15 at a similar fraction of its 0.12 pc core radius (Lauer et al. 1991).

4. DYNAMICAL STATE OF THE NUCLEUS

The central properties of the nucleus are characterized by I_0, which we can compute by integrating equation (10) to $0''.273$ and equating the result to the $\hat{m}_V = 15.77$ derived in § 2. We find

$$\mu_0 = -2.5 \log I_0 = 12.84 V_{\rm mag} \text{ arcsec}^{-2} ,$$

corrected for absorption. Following Kormendy & McClure (1993, hereafter KM93), we analytically deproject the Hubble profile (their eq. [3]) and integrate it (their eq. [6]) to obtain $3.7 \times 10^4 L_{V\odot}$ pc^{-3} within the core. A core mass of 9×10^4 $M_\odot$ follows from $M/L = 2.35$ (Carter & Sadler 1990). The corresponding limit on the mass of a central black hole,

$$M_\bullet \lesssim 9 \times 10^4 \, M_\odot ,$$

is the second strictest limit in a galaxy to date and second to M33 (KM93).

The core radius and the nuclear velocity dispersion of Carter & Sadler (1990) also allow us to calculate the relaxation time in the nucleus (Spitzer & Hart 1971):

$$T_r \approx 1 \times 10^7 \text{ yr.}$$

A pessimistic estimate of the core collapse time ($330T_r$) is significantly less than a Hubble time. Core collapse has therefore possibly taken place, as it has arguably done in a number of galactic globular clusters with even shorter relaxation times (Djorgovski 1993).

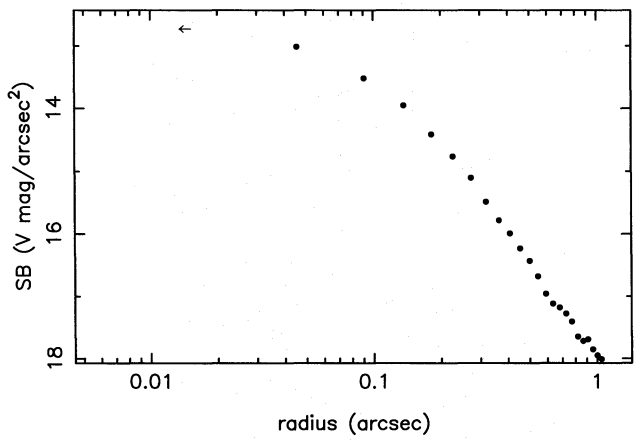

FIG. 7.—The major axis profile that results from a formal deconvolution of the nucleus with 20 Lucy-Richardson iterations. The arrow symbol signifies a central value of the profile.

TABLE 1

DECONVOLVED PROFILE

log r	μ_V
$\lesssim -1.8$	12.73
-1.34	13.01
-1.04	13.52
-0.86	13.95
-0.74	14.41
-0.64	14.76
-0.56	15.10
-0.50	15.49
-0.44	15.78
-0.39	15.99
-0.34	16.23
-0.30	16.43
-0.26	16.68
-0.23	16.96
-0.20	17.12
-0.17	17.18
-0.14	17.28
-0.11	17.41
-0.09	17.65
-0.06	17.72
-0.04	17.69
-0.02	17.85
0.00	17.95
0.02	18.01
0.04	18.28
0.06	18.17

5. DISCUSSION

In the previous section we briefly discussed the similarity we find between the NGC 205 nucleus and a bright globular cluster in terms absolute visual magnitude and possible dynamical history. Figure 8 shows where the M_V and r_c we measure for NGC 205 lie in the relevant distributions for the galactic globular clusters listed by Djorgovski (1993). A detailed comparison of the surface brightness profile of this nucleus with those of galactic globular clusters is beyond the scope of this paper, but clearly there are core collapsed (power-law) clusters with sharper profiles than Figure 7 and conventional King model clusters, which are flatter. We also note that both Carter & Sadler (1990) and Peterson & Caldwell (1993) report a nuclear velocity dispersion of 14–15 km s^{-1} for NGC 205, which is similar to those of the galactic globular clusters in Pryor & Meylan (1993).

The spectrum of the nucleus taken by Da Costa & Mould (1988) shows characteristics, in particular strong hydrogen lines, similar to those seen in the spectra of young globular clusters in the Magellanic Clouds. As noted by Da Costa &

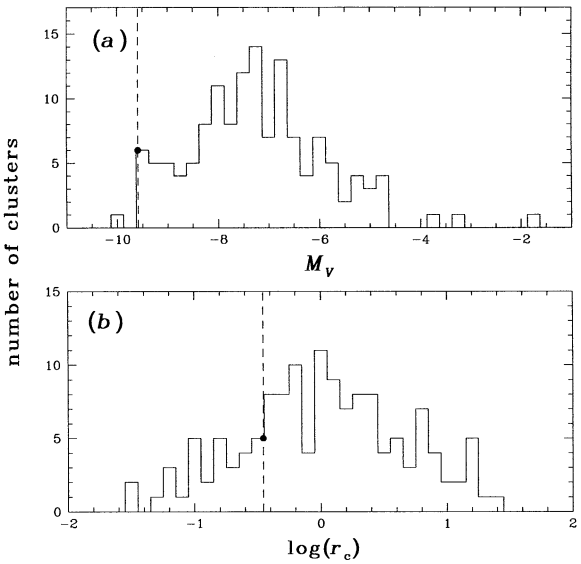

FIG. 8.—Distributions of the known galactic globular clusters in terms of (*a*) absolute visual magnitude M_V, and (*b*) logarithm of core radius. The corresponding values we have measured for the NGC 205 nucleus are denoted by the dashed lines. Data for the globular clusters were taken from the catalog of Djorgovski (1993).

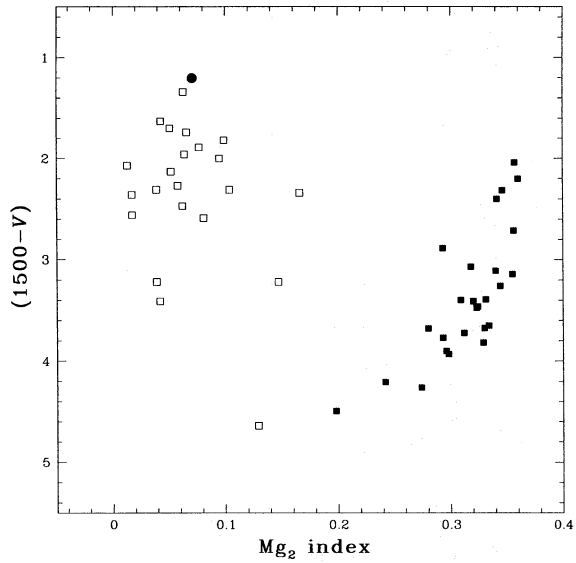

FIG. 9.—(1500 − *V*) vs. Mg_2 line absorption index for galaxies (*solid squares*) and globular clusters (*open squares*) as presented by Dorman et al. (1995). The data for NGC 205 (*solid circle*) are derived from the Mg_2 index listed in Burstein et al. (1988) and the F160BW and F555W photometry in this paper.

Mould (1988), the spectrum of the nucleus is similar to that of the globular cluster Hubble V also in NGC 205. The hydrogen line strength of these two objects is more than twice that of the mean of the other clusters. According to the models of Worthey (1994) a factor of 2.5 increase in Hβ corresponds (at [Fe/H] = −0.25) to an order of magnitude younger age.

We can use the aperture-limited photometry of § 2.3 to derive a (1500 − *V*) color[12] of 1.20 mag. This agrees with the value measured by Burstein et al. (1988). Figure 9 shows a graph of (1500 − *V*) against Mg_2 absorption line strength index from the data in Dorman, O'Connell, & Rood (1995) for a number of nearby galaxies and globular clusters. With a Mg_2 index of 0.017 ± 0.007 mag (Burstein et al. 1988), NGC 205 is placed among the globular clusters in this plot, suggesting that the origin of the hot stellar population in the nucleus may be the same as it is in globular clusters. The corresponding metallicity determined from the relation in Dorman et al. (1995) is [Fe/H] = −1.44; also typical of the galactic globular clusters in Dorman et al. (1995), but lower by 0.6 dex than the mean metallicity found by Mould et al. (1984) for the stars in an off-center NGC 205 field. However, it is possible that the value of Mg_2 has been diluted by the light from young stars at the center of NGC 205. Models by Dorman et al. (1995) are able to fit the (1500 − *V*) colors of old clusters; however, these authors also remark that without an accurate physical prescription for connecting mass loss to age and abundance the (1500 − *V*) colors cannot be used to infer these.

Tremaine, Ostriker, & Spitzer (1975) have modeled the decay of globular cluster orbits due to dynamical friction (minor modifications of which have been suggested by White 1976). They define a unit time for orbit decay of $\tau = \alpha^2\sigma/Gm$, where α is the structural length of the galaxy [=(galaxy core radius)/3], σ is the line-of-sight velocity dispersion for the galaxy and m is the mass of the cluster. Applying this to NGC 205, the nucleus has $M_V = -9.6$, which implies an intrinsic luminosity of $L = 5.7 \times 10^5\ L_\odot$ or a mass of $1.3 \times 10^6\ M_\odot$, (using $M/L = 2.35$; Carter & Sadler 1990).[13] Adopting also a halo velocity dispersion of ~ 50 km s^{-1} for the galaxy and core radius 120 pc (=35″; Carter & Sadler 1990), then $\tau \sim 8 \times 10^7$ yr. In the models of Tremaine et al. (1975), clusters with typical energies per unit mass of several times their σ^2 take an order of magnitude longer than the timescale τ to decay into the core. However, this is still less than a Hubble time and does not discount cluster orbit decay as a plausible explanation for the formation of the nucleus.

We have resolved the nucleus of NGC 205 and shown that it shares the far-ultraviolet upturn measured for NGC 205 by Burstein et al. (1988).

There are a number of possible origins for a structure of this kind.

1. An old nuclear star cluster approximately coeval with the formation of the galaxy.

2. A star cluster (or clusters) similar to the nine well-studied globular clusters of NGC 205, whose orbit has decayed so that it occupies the nuclear location.

3. A cluster formed as the repository of the gas from generations of ongoing star formation in the galaxy (see, e.g., Kormendy & Djorgovski 1989; Kormendy & Richstone 1995, and references therein).

4. A cluster whose predominant population is that of the current burst of star formation in the galaxy.

The strength of the hydrogen lines in the center of NGC 205 does not seem to favor the first or the last hypotheses. On the one hand the optical spectrum suggests that the nucleus of NGC 205 is markedly younger than the stellar

[12] On 1994 October 19 the nucleus of M32 was observed on the WF3 chip of WFPC2, in the same way as NGC 205. It is a weak source yielding only 0.03 e$^-$ s^{-1} in a 2 pixel radius aperture. This implies a 1550 − *V* color 4.7 ± 0.2 mag redder than the nucleus of NGC 205. Burstein et al. (1988) find 1550 − *V* (M32-N205) = 3.2 mag. M32's FUV flux is therefore weaker relative to NGC 205 in the nucleus than in the IUE aperture.

[13] As distinct from their 1″.1 core radius measurement for the nucleus.

population of the halo of the galaxy (Da Costa & Mould 1988; Mould et al. 1984). On the other hand, the optical spectrum is characteristic of stellar populations whose age is of order a billion years, rather than the 10^7 or 10^8 yr of the B supergiants of Baade (1951). The first hypothesis might be saved by postulating a change in the stellar population resulting from core collapse (KM93). The short star-star collision time in the nucleus is likely to favor the formation of blue stragglers with stronger hydrogen lines than old main-sequence stars. However, the integrated spectrum of core-collapsed Galactic globular clusters is not known to be peculiar in this way.

Under the second hypothesis, the origin of the UV upturn in the nucleus is similar to that of the UV upturn in Galactic globular clusters, and it is supposed that mass loss processes in evolved stars are such that the few billion year old simple stellar population (Renzini & Buzzoni 1986) of the cluster still produces hot remnants of late-stage evolution. Only a small sample of Magellanic Cloud clusters is available to test that proposition (de Boer 1981).

The third hypothesis supposes that the nucleus of NGC 205 has been subject to continuous star formation. The UV upturn would then reflect a significant contribution from young stars. This is the essence of the star formation history of the model calculated by Bertola et al. (1995). If the nucleus shares this declining star formation rate plus a burst, the similarity of the subarcsecond and larger aperture colors has a natural explanation. More critical observations would compare the nuclear and off-nuclear colors. Off-nuclear measurements would require higher signal-to-noise observations than we have presented here.

A better understanding of the rich star formation history of this galaxy and its central star cluster awaits full multicolor observations with WFPC2.

We would like to thank Gary Da Costa and Tim de Zeeuw for useful comments on many aspects of this work and John Kormendy for generous discussions of the dynamical state of the nucleus. One of us (D. H. J.) acknowledges the financial support of a Commonwealth Australian Postgraduate Research Award. This research was carried out by the WFPC2 Investigation Definition Team for JPL and was sponsored by NASA through contract NAS7-1260.

REFERENCES

Baade, W. 1951, Publ. Univ. Michigan Obs., 10, 7
Bertola, F., Bressan, A., Burstein, D., Buson, L. M., Chiosi, C., & di Serego Alighieri, S. 1995, ApJ, 438, 680
Bingelli, B., Sandage, A., & Tamınann, G. A. 1985, AJ, 90, 1681
Burrows, C. J., ed. 1994, Wide Field and Planetary Camera 2 Instrument Handbook (Baltimore: STScI)
Burstein, D., Bertola, F., Buson, L. M., & Lauer, T. R. 1988, ApJ, 328, 440
Burstein, D., & Heiles, C. 1984, ApJS, 54, 33
Cardelli, J. A., Clayton, G. C., & Mathis, J. S. 1988, ApJ, 329, L33
———. 1989, ApJ, 345, 245
Carter, D., & Sadler E. 1990, MNRAS, 245, 12P
Da Costa, G., & Mould, J. 1988, ApJ, 334 159
de Boer, K. S. 1981, in Astrophysical Parameters for Globular Clusters, ed. A. G. Davis Philip & D. S. Hayes (New York: Davis), 3
Djorgovski, S. 1993, in ASP Conf. Ser. 50, Structure and Dynamics of Globular Clusters, ed. S. G. Djorgovski & G. Meylan (San Francisco: ASP), 373
Dorman, B., O'Connell, R. W., & Rood, R. T. 1995, ApJ, 442, 105
Gallagher, J., & Mould, J. 1981, ApJ, 244, L3
Held, E., Mould, J., de Zeeuw, T., & Picard, A. 1990, AJ, 100, 415
Hodge, P. 1989, ARA&A, 27, 139
Holtzman, J. 1995, private communication
Holtzman, J. A., Burrows, C. J., Casertano, S., Hester, J. J., Trauger, J. T., Watson, A. M., & Worthey, G. 1995a, PASP, 107, 1065
Holtzman, J. A., Hester, J. J., Casertano, S., Trauger, J. T., Watson, A. M., & WFPC2 IDT. 1995b, PASP, 107, 156
King, I. R. 1966, AJ, 71, 64
Kormendy, J. 1985, ApJ, 295, 73
Kormendy, J., & Djorgovski, S. 1989, ARA&A, 27, 235
Kormendy, J., & McClure, R. 1993, AJ, 105, 1793 (KM93)
Kormendy, J., & Richstone, D. 1995, ARA&A, 33, 581
Krist, J. E., & Burrows, C. J. 1995, Appl. Opt., 34, 4951
Lauer, T. R., et al. 1991, ApJ, 369, L45
Lauer, T. R., et al. 1992, AJ, 104, 552
Lauer, T. R., et al. 1993, AJ, 106, 1436
Mould, J., Kristian, J., & Da Costa, G. S. 1984, ApJ, 278, 575
Nilson, P. 1973, Uppsala General Catalogue of Galaxies (Uppsala: R. Soc. Sci. Uppsala)
Peterson, R. C., & Caldwell, N. 1993, AJ, 105, 1411
Pryor, C., & Meylan, G. 1993, in ASP Conf. Ser. 50, Structure and Dynamics of Globular Clusters, ed. S. G. Djorgovski & G. Meylan (San Francisco: ASP), 357
Renzini, A., & Buzzoni, A. 1986, in Spectral Evolution of Galaxies, ed. C. Chiosi & A. Renzini (Dordrecht: Reidel), 195
Sandage, A., Binggeli, B., & Tammann, G. 1985, AJ, 90, 1759
Spitzer, L., & Hart, M. 1971, ApJ, 164, 399
Trauger, J. T., & WFPC2 IDT. 1994, ApJ, 435, L3
Tremaine, S. D., Ostriker, J. P., & Spitzer, L. 1975, ApJ, 196, 407
Watson, A. M., Mould, J. R., Gallagher III, J. S., & WFPC2 IDT. 1994, ApJ, 435, L55
White, S. D. M. 1976, MNRAS, 174, 467
Worthey, G. 1994, ApJS, 95, 107